Evidence for a crystal–amorphous interphase in PVDF and PVDF/PMMA blends

B. R. Hahn, O. Herrmann-Schönherr and J. H. Wendorff
Deutsches Kunststoff-Institut, 6100 Darmstadt, Schlossgartenstr. 6R, West Germany
(Received 23 July 1985; revised 17 September 1986)

Dielectric relaxation studies and absolute small-angle X-ray investigations give evidence that amorphous interlamellar regions in partially crystalline PVDF/PMMA blends consist of two phases: a pure amorphous PVDF phase and a homogeneously mixed PVDF/PMMA phase. The local phase separation which occurs, despite favourable interactions between PMMA and PVDF, is attributed to a PVDF crystal–amorphous interphase which rejects PMMA segments. The thickness of this interphase is found to be of the order of 2.5 nm.

(Keywords: polymer blends; poly(vinylidene fluoride); poly(methyl methacrylate); small-angle X-ray scattering; dielectric relaxation; structure determination; three phase structure; crystal–amorphous interphase)

INTRODUCTION

Recent theoretical considerations[1,2] have led to the conclusion that a crystal–amorphous interphase could exist in lamellar semicrystalline polymers, the properties of which differ from those of a truly amorphous phase. According to these considerations, the formation of the interphase is caused by steric packing problems. The interphase allows for the dissipation of order existing at the crystal surface. We obtained indirect experimental evidence for the existence of such a phase in poly(vinylidene fluoride), PVDF, while studying the dielectric properties of PVDF and of its blends with poly(methyl methacrylate), PMMA[3].

These two polymers are known to be compatible in the molten state for all concentrations, to display a homogeneous phase down to a molecular level over a wide range of temperatures and to be characterized by a lower critical solution temperature which is located well above their decomposition temperatures[5]. The thermodynamical treatment of these blends leads to the conclusion that the homogeneously mixed state should be stable at lower temperatures, in agreement with the experimental finding that it can be transferred into the glassy state provided that the blends contain less than ~ 50 wt% PVDF[6,7].

Samples containing more PVDF or samples which are annealed above their respective glass transition temperatures behave differently. They display a partial crystallization of the PVDF.

It is known from X-ray scattering studies[8] that the amorphous material is located totally within the spherulites in these blends and that it forms the amorphous regions between the PVDF lamellae. One could then expect, for the thermodynamic reasons pointed out above, that the two components remain homogeneously mixed in the amorphous regions. The assumption, that the two components of the blends are thus intimately and homogeneously mixed in the interlamellar regions, seems straightforward; however, it meets with many problems.

In a previous publication[3], concerned with the dielectric properties of PVDF/PMMA blends, we pointed out that the experimentally observed variation of the glass transition temperature with composition does not agree with this assumption. We proposed a partial phase separation to take place in the disordered interlamellar regions and we related this fact to the existence of an amorphous–crystal PVDF interphase, the thermodynamic properties of which differ from those of the bulk amorphous state.

The formation of the interphase was considered to be an intrinsic property of lamellar PVDF crystals, since PVDF chains are known to contain considerable amounts of head-to-head and tail-to-tail defects[9] occurring in a significant fraction of interphase regions. Such an interphase can be expected to expel a second component, the PMMA component in this case, despite its favourable interaction with PVDF. This gives rise to a two phase amorphous region in partially crystalline blends of PVDF and PMMA.

In this paper we present additional experimental X-ray and dielectric relaxation results, which, in our opinion, are strongly in favour of the existence of such a crystal–amorphous interphase in PVDF and which point out the influence of such an interface on structural and dynamical properties of blends, or at least of the materials considered here.

EXPERIMENTAL

Samples

The PVDF samples were obtained from the Solvay Company. The number- and weight-average molecular weights are known to be $M_n = 38\,000\,\mathrm{g\,mol^{-1}}$ and $M_w = 100\,000\,\mathrm{g\,mol^{-1}}$ respectively. The PMMA samples were obtained from Röhm GmbH and the molecular

0032-3861/87/020201-08$03.00

weights were $M_n = 60\,000\,g\,mol^{-1}$ and $M_w = 120\,000\,g\,mol^{-1}$, respectively. The two polymers were melt blended at 220°C in an extruder. Thin films with a thickness ranging between 40 μm and 60 μm were extruded from these mixtures. All films were found to be macroscopically homogeneous and to exhibit excellent optical clarity. Aluminium electrodes of 100 nm in thickness and 2.1 cm in diameter were vapour deposited onto both sides of the films for dielectric investigations.

X-ray studies

Wide-angle and small-angle diagrams were obtained by means of a Siemens wide-angle goniometer and a Kratky small-angle X-ray camera, using CuKα radiation of wavelength 0.154 nm. The absolute intensity was established by comparing the scattering intensity of the samples with that of a calibration sample. The scattering curves were desmeared, using a procedure developed by Strobl[10]. The analysis of the scattering curves will be discussed in detail below.

Dielectric measurements

The dielectric properties were measured using a General Radio bridge (type 1616). The samples were placed in an environmental chamber under dry helium atmosphere. The temperature was increased linearly at a rate of 2 K min^{-1} from −140°C to 150°C and the bridge was balanced manually.

I.r. measurements

I.r. spectra were obtained using a Perkin Elmer (type 598) spectrometer.

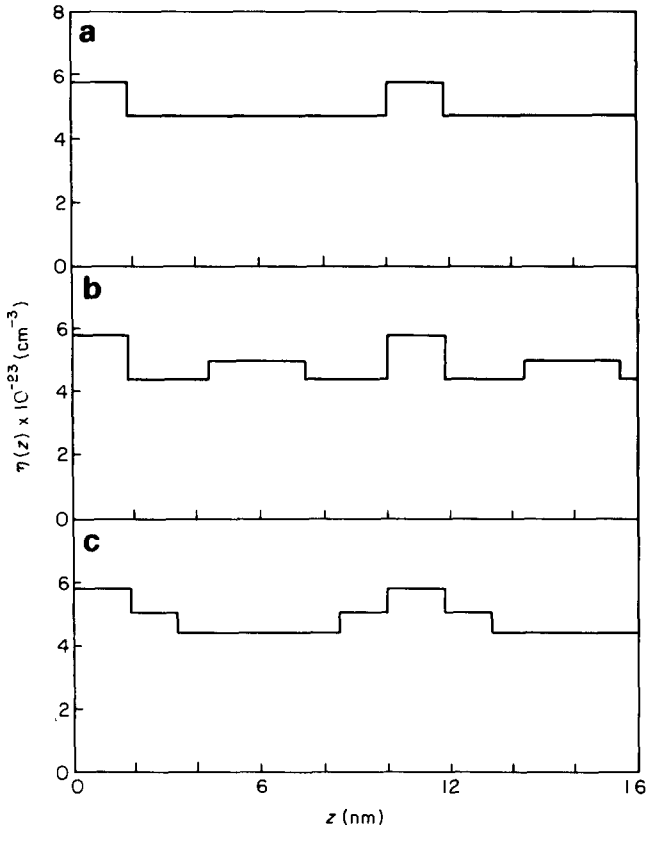

Figure 1 Models of one dimensional electron density distributions of the unannealed PVDF/PMMA blend with 20 wt % PMMA and 80 wt % PVDF as explained in the text

RESULTS AND DISCUSSION

Small-angle X-ray scattering results

It was already pointed out above that PMMA was found to be located within the spherulites in partially crystalline blends of PMMA and PVDF and furthermore that PMMA is located within the amorphous regions between the PVDF lamellae[13,14]. It is clear that one has to expect totally different density (and thus electron density) distributions for the case of a one phase amorphous region or a two phase amorphous region, which, in turn, may be structured in two different ways (*Figure 1*):

(a) a two phase model with a homogeneously mixed amorphous one phase region;

(b) a three phase model with amorphous PVDF regions located in the interior of the interlamellar regions;

(c) a three phase model with amorphous PVDF as a crystal–amorphous interphase.

Absolute small-angle X-ray studies should be able to discriminate between the various models which are, of course, idealized models. The expectation is that the interface becomes increasingly accessible to the PMMA chains as the distance from the surface of the crystal increases. One could thus envisage a gradual increase in the PMMA concentration with increasing distance from the crystal surface.

The dielectric relaxation studies, reported in a previous publication[3], however, contradict this assumption. The location of the dielectric relaxation peak, which occurs below 0°C and which is attributed to the glass relaxation within the disordered regions of PVDF, was found to be independent of the PMMA concentration. Its strength, on the other hand, decreased with increasing PMMA content. The conclusion is that there seems to be a rather well defined interfacial layer which totally excludes PMMA. We cannot exclude, of course, the possibility of a transition layer between the disordered PVDF phase and the amorphous PVDF/PMMA regions. Its extent is, however, clearly small in comparison with that of the interfacial layer and we will neglect it for this reason. In any case, it will be difficult to decide from the X-ray data whether this small transition layer is present or not.

In the following we will assume that the density variations occur predominantly along the direction perpendicular to the lamellae, as long as we stay within an lamellar aggregate. Therefore, we are able to restrict our discussion to one dimensional density correlation functions $K(z)$, where z points appear along the layer normal.

$$K(z) = 2\pi^2 \langle [\eta(z') - \langle \eta \rangle][\eta(z'+z) - \langle \eta \rangle] \rangle \qquad (1)$$

η is the electron density and the angular brackets indicate averaging over all coordinates z' within a lamellar aggregate. This function was evaluated from the desmeared small-angle scattering curve $I(s)$:

$$K(z) = \int_0^\infty I(s) s^2 \cos(sz) ds \qquad (2)$$

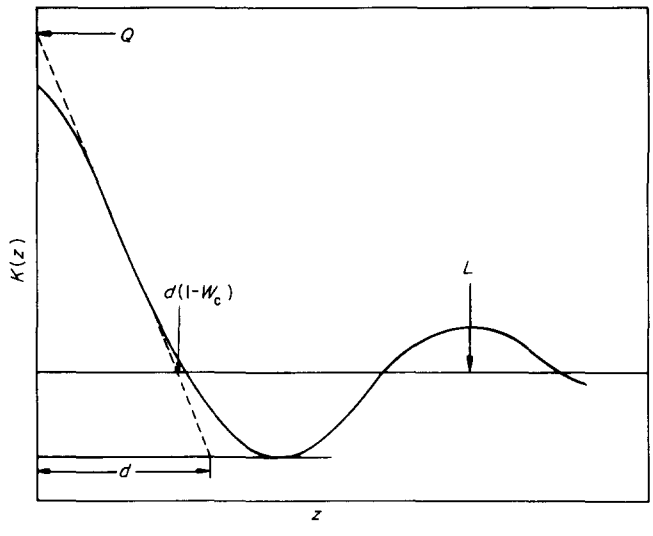

Figure 2 General properties of the electron density correlation function of a partially crystalline polymer. The analysis permits a direct determination of the mean crystallite thickness d, the most probable long spacing L and the invariant Q (Strobl *et al.*[15])

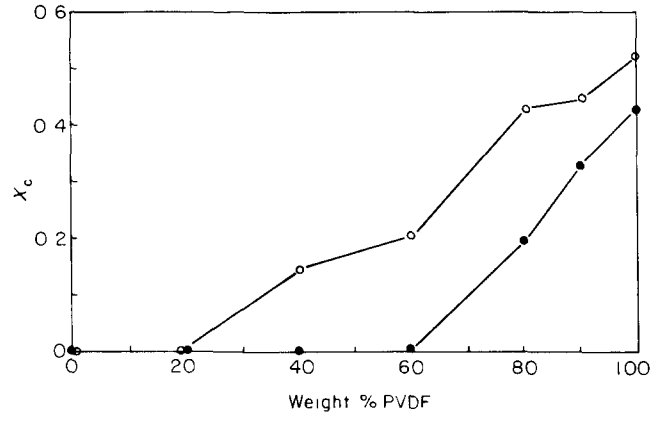

Figure 3 Degree of crystallinity X_c of PVDF/PMMA blends as a function of the composition: (○) samples annealed at 135°C for 24 h; (●) unannealed samples

s denotes the scattering vector

$$s=\frac{4\pi}{\lambda}\sin\theta \tag{3}$$

where λ is the wavelength and θ is the Bragg-angle. The assumptions on which this approach is based as well as the structural information which can be derived from this correlation function have been discussed in detail by Strobl *et al.*[15]. *Figure 2* gives a schematic representation of such a correlation function for a two phase structure, characterized by average electron densities allowing for interfacial regions and variations in the thickness of the crystalline lamellae and the amorphous regions. One obtains the following structural parameters: the average thickness d of the lamellae, the long spacing value L and the magnitude of the invariant Q.

$$Q=2\pi^2 w_c(1-w_c)(\eta_c-\eta_a)^2 \tag{4}$$

w_c is the degree of crystallinity and η_c and η_a are the average electron densities of the crystalline and amorphous regions, respectively.

It is important for the following analysis to know the structure of the two components. PMMA poses no problem since it is totally amorphous and the small-angle intensity is mainly determined by thermal density fluctuations[4]. PVDF is partially crystalline with a degree of crystallinity of about 50%[11]. Wide-angle X-ray studies have revealed that the degree of crystallinity of the blends depends both on the composition and on the thermal treatment of the samples. Untreated samples showed no traces of crystallinity for blends containing less than 60 wt% PVDF. This is shown in *Figure 3*. The degree of crystallinity increases almost linearly with increasing PVDF content above this critical concentration. Well annealed samples, however, were characterized by a critical concentration of about 20 wt% PVDF, above which the degree of crystallinity increased also with increasing PVDF content.

PVDF is known to be able to display several crystal modifications[11], the most prominent being the polar β-modification and the nonpolar α-modification. The relative amount of the two modifications present in the blends was determined by i.r. studies. The α-modification displays characteristic absorption bands at 531 cm^{-1} and 410 cm^{-1} whereas the corresponding absorption bands for the β-modification are located at 508 and 441 cm^{-1} respectively[12]. Some of the i.r. spectra obtained for the blends are given in *Figure 4*. The concentration of the β-modification increases with increasing concentration of PMMA relative to the total degree of crystallization. We will use these results in detail later.

These morphological data are used below in the analysis of the small-angle X-ray scattering curves. To start with, we tested whether the absolute small-angle X-ray results obtained for pure PVDF samples agree with the theoretical predictions, based on a two phase structure.

Figure 5 shows the smeared small-angle scattering curves for PVDF at 22°C and 100°C, as obtained experimentally. The scattering intensity increases with increasing temperature because of increasing differences in density between the amorphous and crystalline regions. After desmearing and background corrections we obtained the correlation functions shown in *Figure 6*. The structure parameters derived from these curves are given in *Table 1*.

Using the data on the densities of the amorphous and the crystalline regions of PVDF as a function of

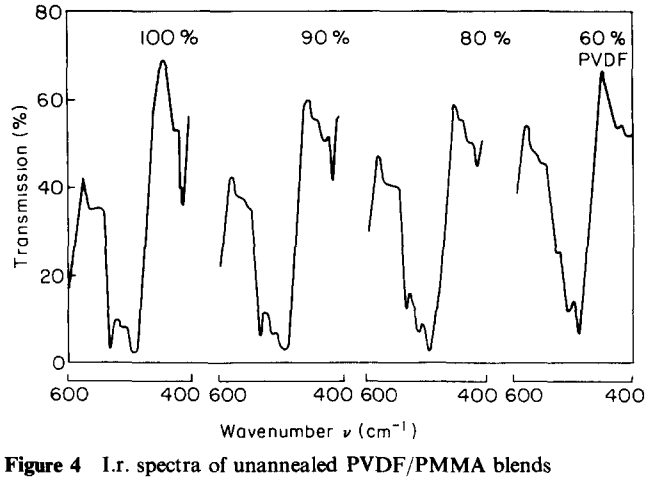

Figure 4 I.r. spectra of unannealed PVDF/PMMA blends

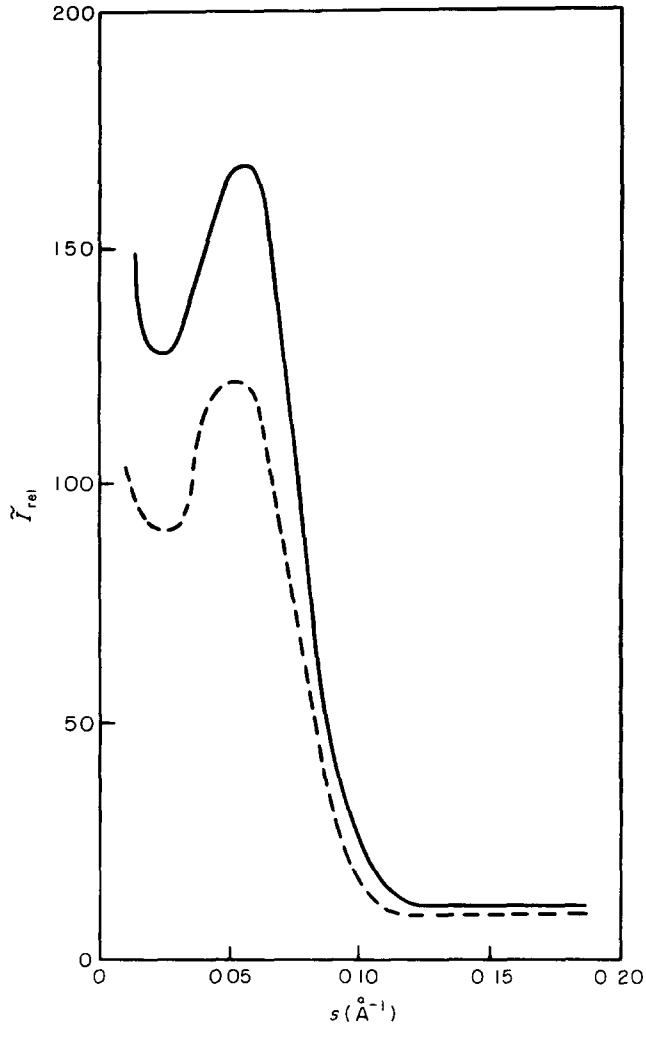

Figure 5 Slit-smeared SAXS curves $\tilde{I}_{rel}(s)$ of PVDF in relative units: (---) 22°C; (———) 100°C

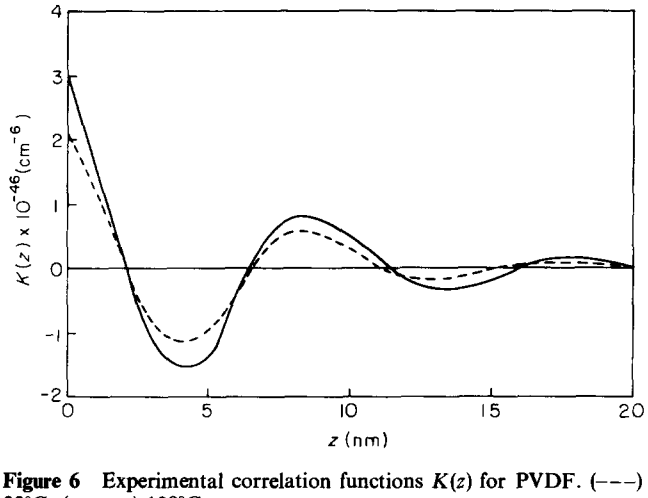

Figure 6 Experimental correlation functions $K(z)$ for PVDF. (---) 22°C; (———) 100°C

temperature, as given by Nakagawa and Ishida[16], we predicted the invariants to be

$$Q = 2.1 \times 10^{46}\ \text{cm}^{-6} \text{ at } 22°\text{C}$$

and

$$Q = 3 \times 10^{46}\ \text{cm}^{-6} \text{ at } 100°\text{C}$$

in excellent agreement with the experimental data. This result shows that this method of analysis yields reliable data.

Next we will discuss the small-angle X-ray results obtained for partially crystalline blends of PMMA and PVDF. *Figure 7* shows the scattering diagram for unannealed and annealed samples, containing between 10 and 40 wt% PMMA. One observes that the scattered intensity increases with increasing PMMA content, due to the increase of the density contrast between the crystalline and the amorphous regions. One can also observe that the long period is shifted to larger values, since PMMA is contained in the interlamellar regions. Annealed samples display larger values of the scattered intensity than the unannealed samples, since annealing leads to a larger degree of crystallinity.

Figure 8 shows the one dimensional correlation functions obtained from these scattering curves. Their shapes agree quite well with those observed for pure PVDF. The invariant increases with increasing PMMA content and is larger in annealed samples as compared with untreated samples for the reasons discussed above.

We will now analyse the information derived from these correlation functions along the same lines used above for pure PVDF. One straightforward result is that the experimentally determined invariants and those calculated from the known densities of amorphous and crystalline PVDF and of PMMA do not agree. The experimentally observed invariants are definitely larger than those calculated (*Figure 9*).

Table 1 Structure parameters of PVDF obtained from one dimensional correlation functions

T (°C)	Q (10^{46} cm^{-6})	d (nm)	L (nm)
22	2.1	3.6	8.5
100	3.0	3.6	8.5

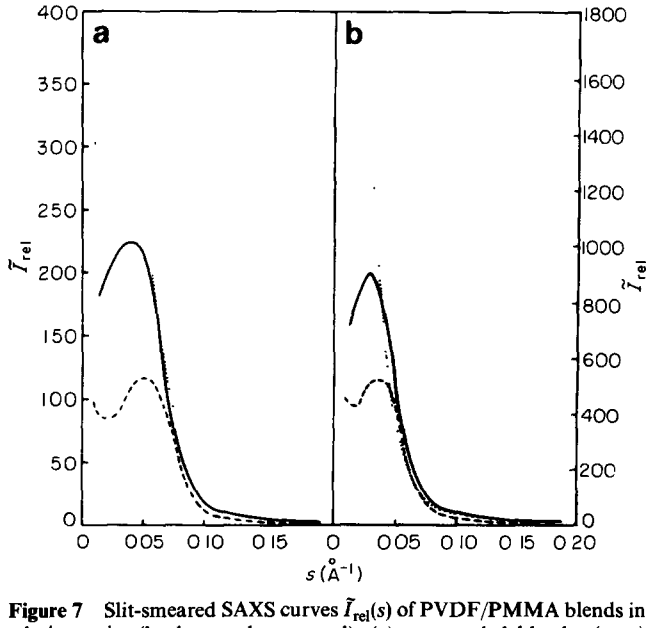

Figure 7 Slit-smeared SAXS curves $\tilde{I}_{rel}(s)$ of PVDF/PMMA blends in relative units (background corrected). (a) unannealed blends: (---) 100 wt% PVDF; (———) 90 wt% PVDF; (·····) 80 wt% PVDF. (b) annealed samples: (---) 90 wt% PVDF; (———) 80 wt% PVDF; (·····) 60 wt% PVDF

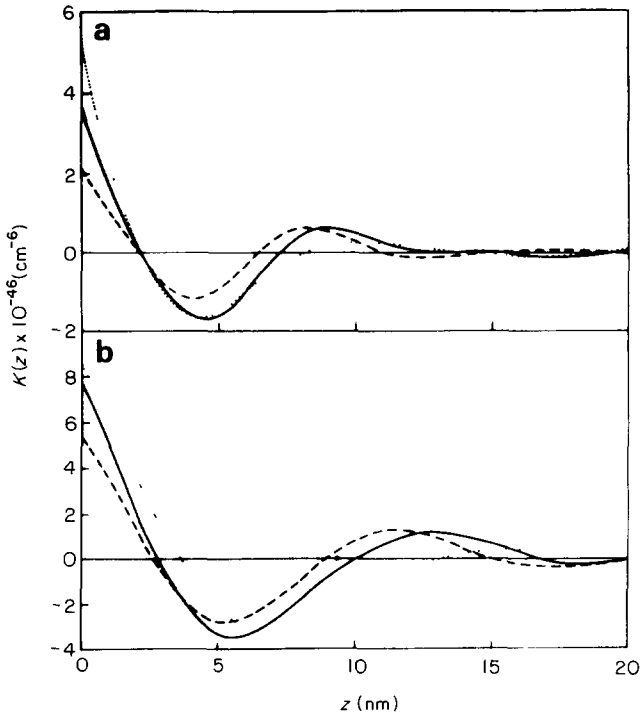

Figure 8 Experimental correlation functions obtained for PVDF/PMMA blends. (a) unannealed blends: (– – –) 100 wt% PVDF; (———) 90 wt% PVDF; (· · · · ·) 80 wt% PVDF. (b) annealed samples: (– – –) 90 wt% PVDF; (———) 80 wt% PVDF; (· · · · ·) 60 wt% PVDF

The blends pose a particular problem because they display different crystalline modifications. Therefore we are forced to determine the average crystalline electron density η_c by

$$\eta_c = \eta_\beta w_\beta + \eta_\alpha(1 - w_\beta) \tag{5}$$

where the volume fraction w_β of the β-modification was determined from the i.r. spectra.

The disagreement between calculated and observed values of the invariants cannot be attributed to uncertainties in the average crystalline density. The calculated invariants stay below the experimental invariants even if we use the density η_β of the β-modification rather than η_c. The density η_β is well above the corresponding value η_α of the α-modification[17] and hence well above η_c. Furthermore, we found that we had to vary the degree of crystallinity by 50% in order to get an agreement between calculated and experimental data. This is well above the range of uncertainties. Therefore, we concluded that the partially crystalline state of the blends cannot be treated as a two phase state. We assumed, as discussed earlier, a three phase state, consisting of crystalline regions, an amorphous interphase containing pure PVDF and a mixed amorphous phase containing PMMA. The invariant is then given by[18]

$$Q = 2\pi^2[w_c w_a(\eta_c - \eta_a)^2 + w_c w_e(\eta_c - \eta_e)^2 + w_e w_a(\eta_e - \eta_a)^2] \tag{6}$$

The subscripts c, a, e, refer to the crystalline, the homogeneously mixed amorphous region and the pure amorphous PVDF phase, respectively. The analysis shows that the assumption of a three phase state leads to an increase of the calculated invariants relative to those of a two phase state. The variation depends on the composition. We varied the fraction of the pure PVDF amorphous phase and of the mixed amorphous phase. We checked the predicted magnitude of the invariants. The best fit was obtained for the compositions given in *Table 2*. We will compare these predictions with those obtained from a quantitative analysis of the dielectric relaxation studies below.

In addition to analysing the magnitude of the invariant we tried to gain some information on the location of the amorphous PVDF region within the interlamellar region. For this purpose we calculated the one dimensional correlation functions for the models b and c, given in *Figure 1*. Although these are, as pointed out above, rather idealized models, they allow us to obtain qualitative information on the internal structure of the amorphous

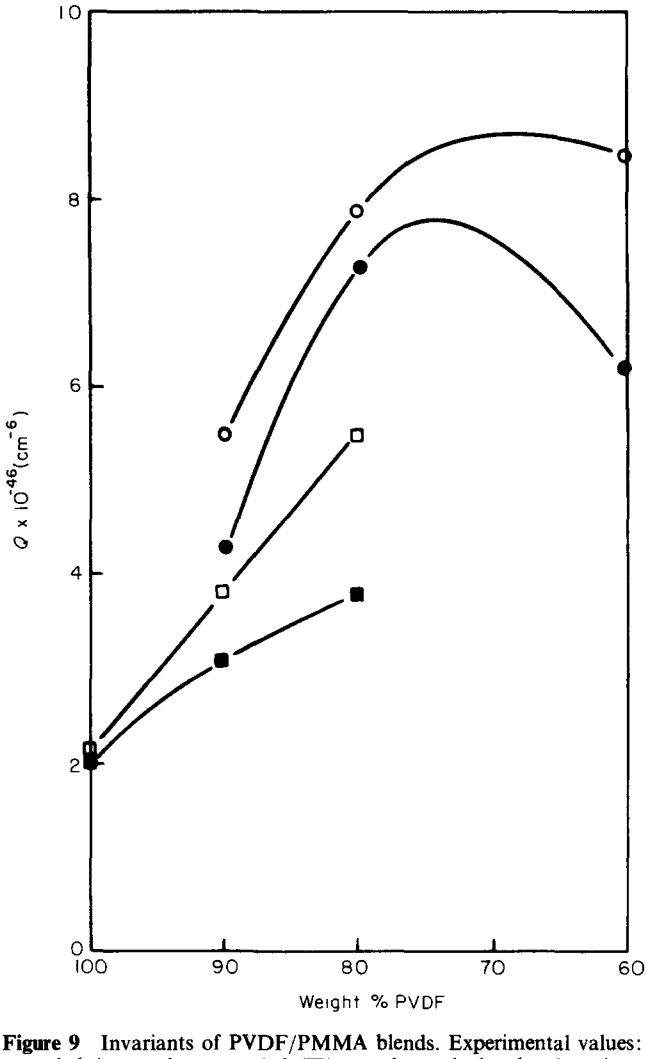

Figure 9 Invariants of PVDF/PMMA blends. Experimental values: annealed (○) and unannealed (□) samples; calculated values (two phase model): annealed (●) and unannealed (■) samples

Table 2 Calculated weight fractions $X_{c,e,a}$ of the various phases in blends of PVDF and PMMA

Weight % PVDF	Unannealed samples			Annealed samples		
	X_c	X_e	X_a	X_c	X_e	X_a
90	0.34	0.33	0.33	0.45	0.33	0.22
80	0.22	0.30	0.48	0.43	0.11	0.46
60	–	–	–	0.22	0.21	0.57

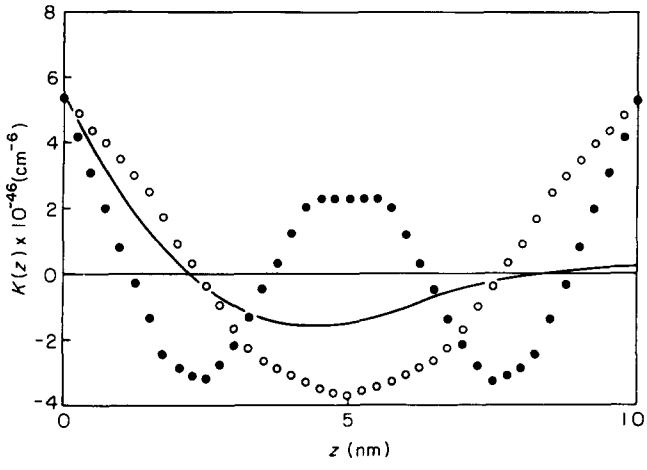

Figure 10 Correlation functions of the unannealed blend with 80 wt% PVDF: (———) experimental; (●) model b; (○) model c

regions. The calculated functions are compared with the experimental function obtained for a blend of 20 wt% PMMA and 80 wt% PVDF in *Figure 10*. The data definitely do not agree with the assumption of an amorphous region consisting of PVDF being located in the interior of the interlamellar regions. The model of an amorphous PVDF interphase which separates the crystalline and the mixed amorphous regions agrees with the experimental finding. This is reasonable in view of the theoretical predictions of the existence of interphases in partially crystalline polymers such as PVDF[2,3].

Dielectric relaxation studies

The dielectric relaxation spectra of blends of PMMA and PVDF, some of which were analysed in a previous paper[3], will be used to obtain additional quantitative information on the internal distribution of the components in partially crystalline blends.

The dielectric relaxation spectra of the blends are depicted in *Figures 11* and *12*. The β-relaxation characteristic of the pure PVDF is observed even for large concentrations of the PMMA component. If one assumes that the two polymers are homogeneously mixed in the amorphous regions of the partially crystalline blends one would expect with increasing PMMA concentration a shift of the glass relaxation to larger temperatures[22]. Yet, one observes that the relaxation occurs in all blends within the same temperature interval. It is just the relaxation strength which decreases continuously with increasing PMMA content. Similar results were obtained for the temperature dependence of the piezoelectric and pyroelectric activities[23]. These activities are known to increase strongly in pure PVDF if the temperature becomes higher than the glass transition temperature. These results suggest again the presence of a disordered PVDF component in addition to a mixed PVDF/PMMA component in the partially crystalline state. In the following we attempt to quantify these statements.

The weight fractions of the PVDF in the crystalline regions X_c, in the interphase regions X_e and in the mixed amorphous regions X_a are related to the total weight fraction X in the blends by

$$X = X_c + X_a + X_e \tag{7}$$

We determined the quantities $X_{c,a,e}$ as follows. The weight fraction X_c of PVDF in the crystalline regions was derived from wide-angle X-ray scattering (*Figure 3*). X_e was determined from the dielectric data. X_a was calculated from equation (7).

The determination of X_a is rather difficult; however, X_e can be obtained by using a relationship given by Fröhlich[19,24] which relates the dipole concentration N and the relaxation strength to the effective mean square dipole moment $\bar{\mu}^2$:

$$\Delta\varepsilon = \frac{4\pi N}{3kT}\bar{\mu}^2\xi \tag{8}$$

The parameter ξ is the ratio of the internal to the external field. Using the Onsager approximation[19] one obtains

$$\xi = \left(\frac{\varepsilon_u + 2}{3}\right)^2 \left(\frac{3\varepsilon_R}{2\varepsilon_R + \varepsilon_u}\right) \tag{9}$$

The determination of $\Delta\varepsilon$ is necessary in order to evaluate N or rather X_a is subject to some errors. For this reason

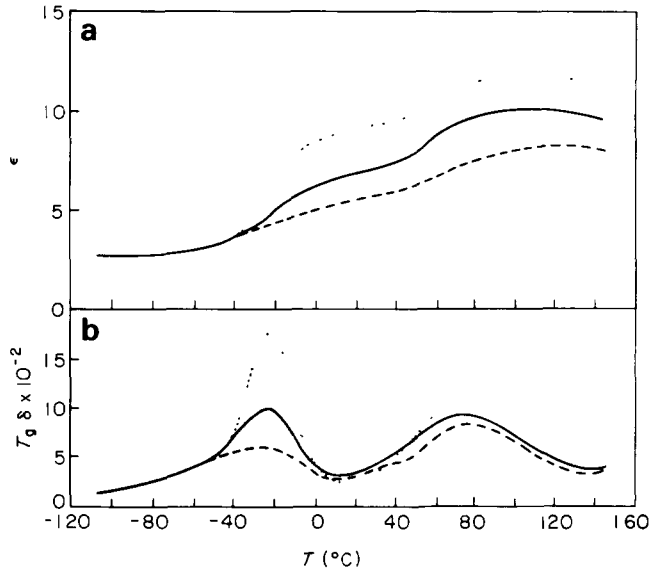

Figure 11 Dielectric constants and tan δ at 1 kHz of PVDF/PMMA blends as a function of temperature: (·····) 100 wt% PVDF; (———) 90 wt% PVDF; (– – –) 80 wt% PVDF

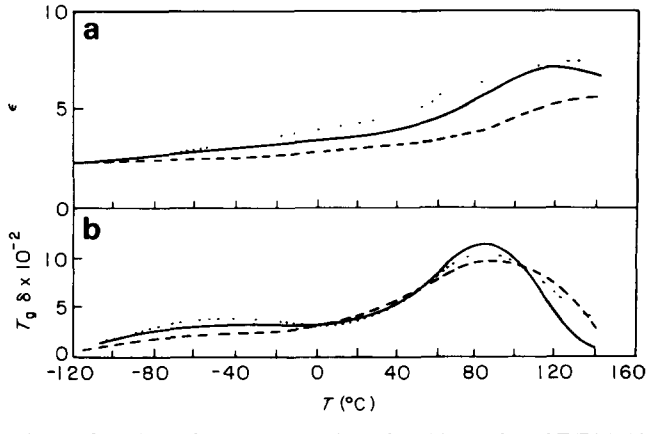

Figure 12 Dielectric constants and tan δ at 1 kHz of PVDF/PMMA blends as a function of temperature: (·····) 60 wt% PVDF; (———) 40 wt% PVDF; (– – –) 20 wt% PVDF

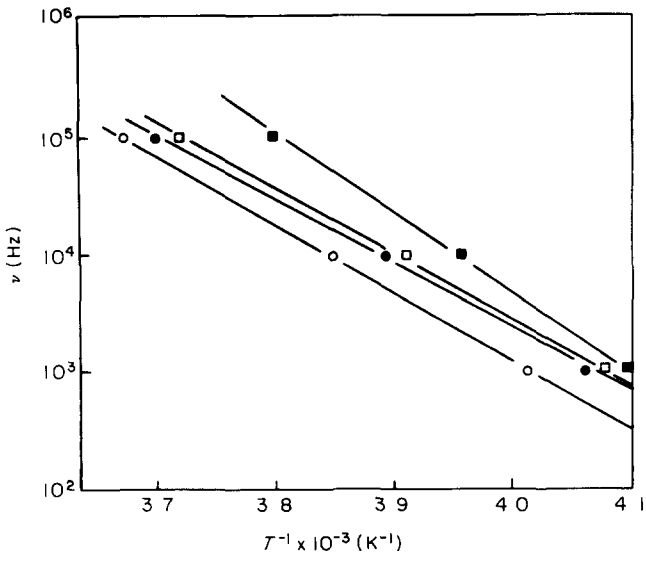

Figure 13 Arrhenius plot (uniaxially oriented blends): (○) 100 wt% PVDF; (●) 90 wt% PVDF; (□) 80 wt% PVDF; (■) 60 wt% PVDF

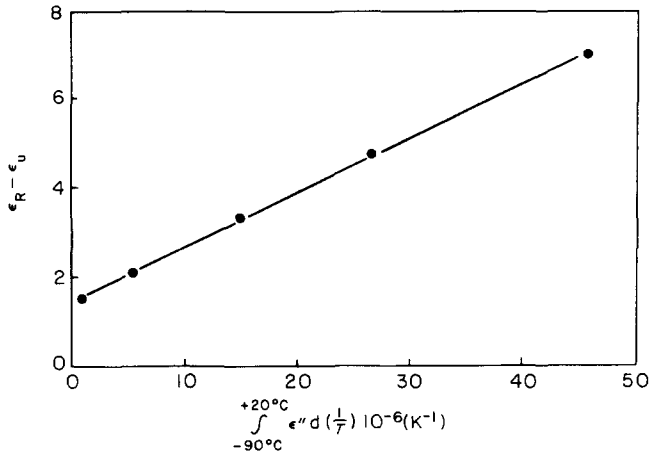

Figure 14 Relaxation strength $\Delta\varepsilon$ plotted as a function of area A under the dielectric loss curve

we used the area A under the dielectric loss curve

$$A = \int \varepsilon'' \mathrm{d}\frac{1}{T} \tag{10}$$

McCrum[25] has shown that the dielectric relaxation strength is related to A via the average activation energy H^{-1}.

$$H^{-1} = \Delta\varepsilon \frac{R}{2}\left(\int \varepsilon'' \mathrm{d}\frac{1}{T}\right)^{-1} \tag{11}$$

One obtains

$$N = \frac{3kTH}{2\pi R\bar{\mu}^2\xi}\int \varepsilon'' \mathrm{d}\frac{1}{T} \tag{12}$$

by combining equations (8) and (11) where R is the gas constant.

The experimental results show that the activation energy for the dipole relaxation process in the PVDF interphase is not influenced by the presence of PMMA.

Figure 13 shows the Arrhenius plot of the frequency shift of the dielectric loss peak obtained on partially crystalline blends (uniaxially oriented samples). The activation energies evaluated from the slopes are 115 and 130 kJ mol^{-1}. *Figure 14* shows a linear relation between $\Delta\varepsilon$ and A giving the same activation energy of 158 kJ mol^{-1} for all partially crystalline blends (isotropic samples), according to equation (11). One observes that the relaxation behaviour of the PVDF interphase seems to be independent of the PMMA fraction. This justifies the assumption that the first part in equation (12) does not depend on the PMMA fraction in the partially crystalline blends. Thus we obtain

$$X_c = B\xi\int \varepsilon'' \mathrm{d}\frac{1}{T} \tag{13}$$

where the constant factor B was derived from the experimentally determined data of X_c, ξ and A for pure PVDF.

The results of these calculations are depicted in *Figure 15* in the form of a phase diagram. It shows the weight fraction of PVDF and PMMA in the mixed amorphous phase and the weight fraction of pure PVDF in the crystalline and the interphase regions for unannealed samples. Similar results were obtained for annealed samples. These results allow us to determine the composition of the mixed amorphous phase as a function of the macroscopical composition of the blends.

We can also analyse the variation of the fraction of the interphase as a function of the fraction of the crystalline regions. The result is that the ratio of the fraction of the interphase and of the crystalline phase has a nearly constant value of 1. The extrapolation to 100 wt% PVDF leads to the prediction that all of the noncrystallized material is located in the interphase. Based on a long period of 8.5 nm (*Table 1*) and a degree of crystallinity of $X_c = 50\%$ we estimate the thickness of the interphase layer to be about 2.0–2.5 nm. The composition of the bulk amorphous phase varies strongly as a function of the overall composition, as is obvious from *Figure 15*. Consequently this is also the case for the corresponding

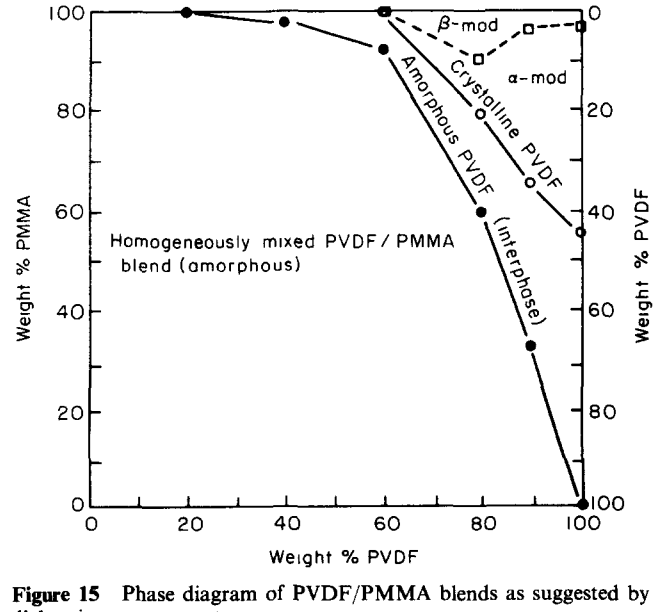

Figure 15 Phase diagram of PVDF/PMMA blends as suggested by dielectric measurements

glass transition of this phase. The experimental determination of this glass transition is difficult because the β-relaxation was found to take place in nearly the same temperature range.

CONCLUSIONS

The structural X-ray investigations as well as the dielectric relaxation studies have revealed that partially crystalline blends of PMMA and PVDF display a crystalline phase, a bulk amorphous phase containing both PVDF and PMMA and, in addition, a crystal–amorphous interphase containing apparently only pure PVDF. The ratio of the crystalline and interphase fractions was found to be about 1. In a previous paper[8] we reported that the lamellar thickness is independent of the composition in partially crystalline PVDF/PMMA blends, provided that the thermal history is kept constant. The amorphous layer was found to increase strongly in thickness with increasing PMMA content. We conclude that the interphase is characterized by a constant width of about 2.0–2.5 nm for the blends considered here.

REFERENCES

1 Flory, P. J., Yoon, D. Y. and Dill, K. *Macromolecules* 1984, **17**, 862
2 Yoon, D. Y. and Flory, P. J. *Macromolecules* 1984, **17**, 868
3 Hahn, B. R., Wendorff, J. H. and Yoon, D. Y. *Macromolecules* 1985, **18**, 718
4 Wendorff, J. H. *J. Polym. Sci., Polym. Lett. Edn.* 1980, **18**, 439
5 Bernstein, R. E., Cruz, C. A., Paul, D. R. and Barlow, J. W. *Macromolecules* 1977, **10**, 681
6 Hirata, Y. and Kotaka, T. *Polym. J.* 1981, **13**, 273
7 Paul, D. R. and Altamirano, J. O. *Adv. Chem. Ser.* 1975, **142**, 371
8 Ullmann, W. and Wendorff, J. H. *Compos. Sci. Technol.* 1985, **23**, 97
9 Görlitz, V. M., Minke, R., Trautvetter, W. and Weisgerber, G. *Makromol. Chem.* 1973, **29/30**, 137
10 Strobl, G. R. *Acta Crystallogr.* 1970, **A26**, 367
11 Lovinger, A. J. in 'Developments in Crystalline Polymers—1', (Ed. D. C. Bassett), Applied Science Publishers, London, 1982
12 Kobayashi, M., Tashiro, K. and Tadokoro, H. *Macromolecules* 1975, **8**, 158
13 Morra, B. S. and Stein, R. S. *Polym. Eng. Sci.* 1984, **24**, 311
14 Morra, B. S. and Stein, R. S. *J. Polym. Sci., Polym. Phys. Edn.* 1982, **20**, 2219
15 Strobl, G. R. and Schneider, M. *J. Polym. Sci., Polym. Phys. Edn.* 1980, **18**, 1343
16 Nakagawa, K. and Ishida, Y. *Kolloid Z. Z. Polym.* 1973, **251**, 103
17 Hasegawa, R., Takahashi, Y., Chatani, Y. and Tadokoro, H. *Polym. J.* 1972, **3**, 600
18 Kratky, O. and Wawra, H. *Monatsh. Chem.* 1963, **94**, 981
19 Nakagawa, K. and Ishida, Y. *J. Polym. Sci., Polym. Phys. Edn.* 1973, **11**, 1503
20 Yano, S. *J. Polym. Sci., Polym. Phys. Edn.* 1974, **12**, 1875
21 Mikhailov, G. P., Borisova, T. I. and Dmitrochenko, D. A. *Sov. Tech. Phys.* 1956, **26**, 1857
22 Couchman, P. R. *Macromolecules* 1980, **13**, 1272
23 Hahn, B. R. and Wendorff, J. H. *Polymer* 1985, **26**, 1611
24 Frölich, H. 'Theory of Dielectrics', Oxford Univ. Press, 1958
25 McCrum, N. G., Read, B. E. and Wiliiams, G. 'Anelastic and Dielectric Effects in Polymeric Solids', J. Wiley, 1967